

1 **Supplementary Material**

2 **Greening of Eurasia's center driven by low-latitude climate**

3 **warming**

4 Shijie Wang^a, Feng Chen^{a,b,c,*}, Youping Chen^a, Max C.A. Torbenson^{d,e}, Jan Esper^{d,e},
5 Xiaoen Zhao^{a,b}, Mao Hu^{a,b}, Heli Zhang^{a,c}, Weipeng Yue^a, Honghua Cao^{a,b}

6 ^a Yunnan Key Laboratory of International Rivers and Transboundary Eco-Security,
7 Institute of International Rivers and Eco-Security, Yunnan University, Kunming,
8 650504, China

9 ^b Southwest United Graduate School, Kunming, 650092, China

10 ^c Key Laboratory of Tree-ring Physical and Chemical Research of the Chinese
11 Meteorological Administration/Xinjiang Laboratory of Tree-ring Ecology, Institute of
12 Desert Meteorology, Chinese Meteorological Administration, Urumqi, 830002, China

13 ^d Department of Geography, Johannes Gutenberg University, Mainz, Germany

14 ^e Global Change Research Institute of the Czech Academy of Science, Brno, the
15 Czech Republic

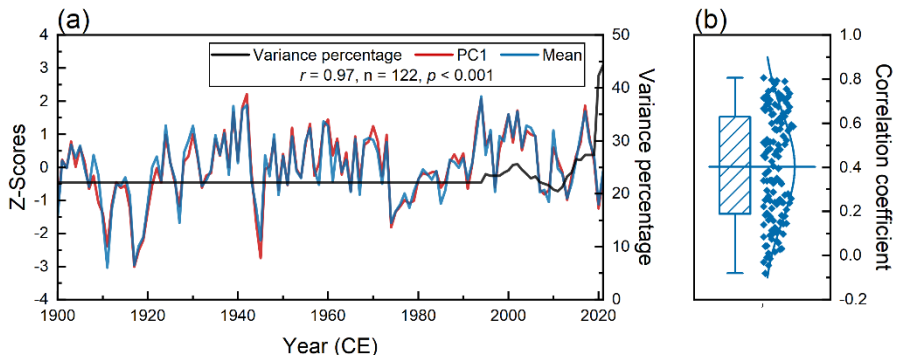
16

17 E-mail address: feng653@163.com (F. Chen)

18

19 This file includes:
20 Supplementary Figures 1-11
21 Supplementary Tables 1-2
22

23



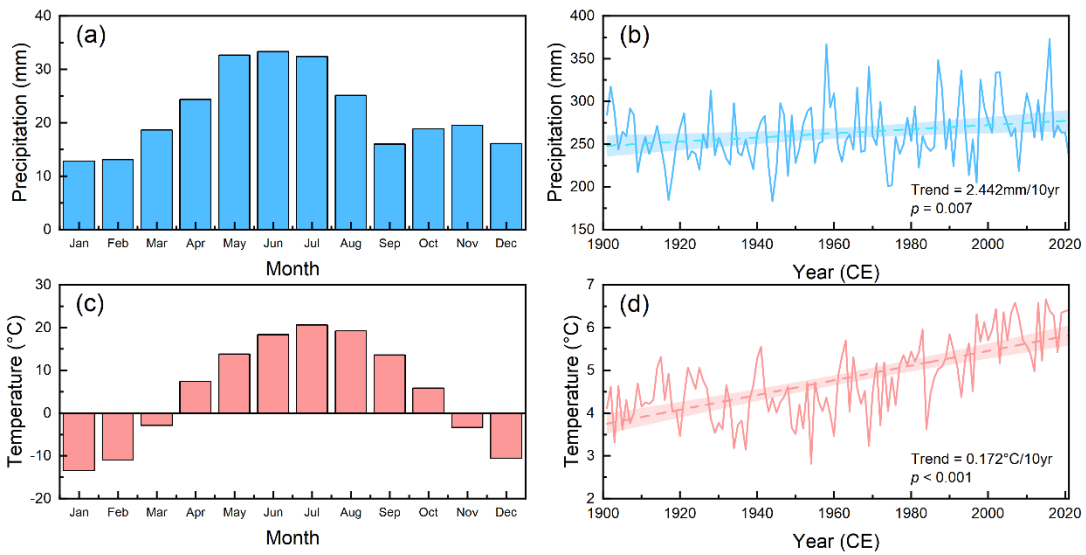
24

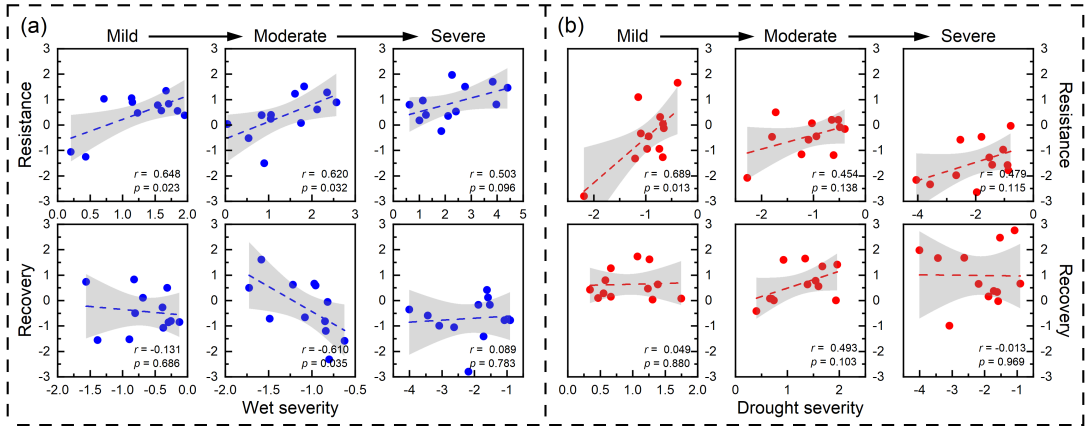
Figure S1. (a) Comparison of nested PC1 vs. mean and variance percent in PC1 for
128 chronologies. (b) Distribution of correlation coefficients for each chronology
with PC1. The box of the box-and-whisker plot represents the 25%–75% range, the
whiskers extend to ± 1.5 times the Interquartile Range (IQR), and the center line
represents the mean. Scatter and normal distribution plots are presented on the right.

29

30

31 **Figure S2.** Monthly **(a)** and annual total **(b)** precipitation from CRU TS4.07 in
 32 Central Asian alpine forests (40° – 50° N, 70° – 90° E) from 1901 to 2021. **(c)** and **(d)** are
 33 the same as **(a)** and **(b)**, respectively, but for monthly and annual mean temperatures.
 34 The dashed lines represent linear fits, while the shaded areas denote the 95%
 35 uncertainty ranges.
 36

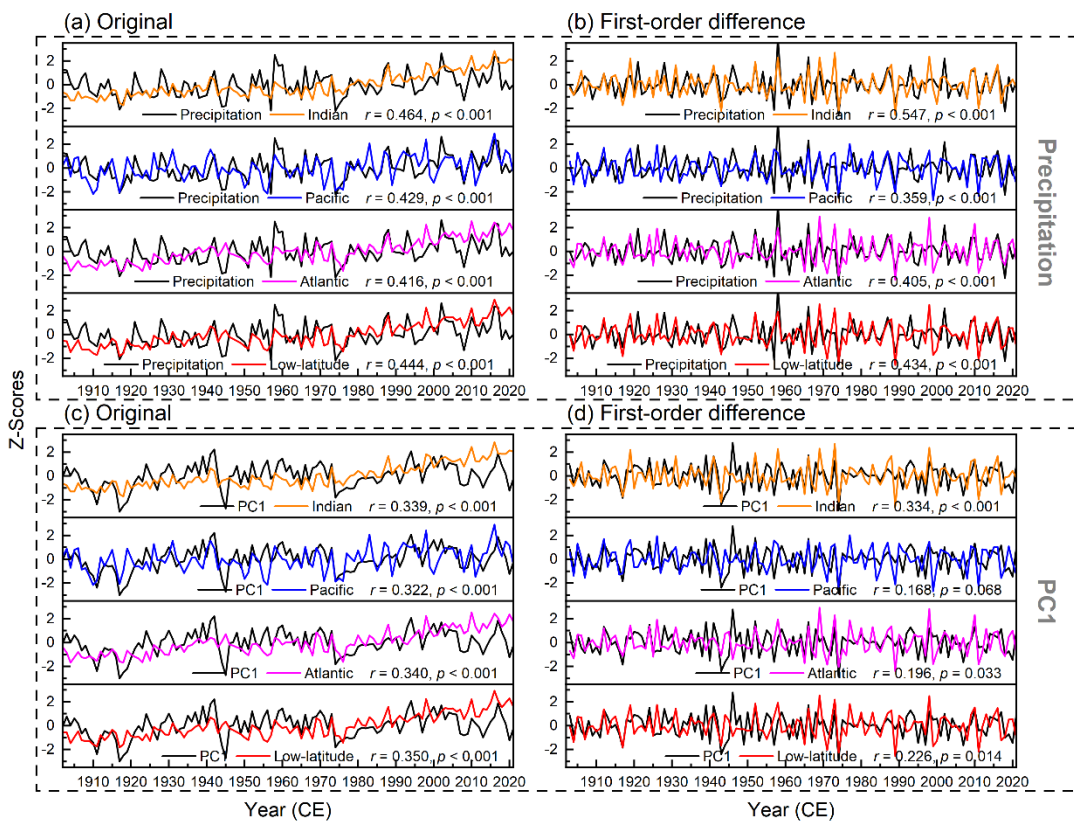




37

38 **Figure S3.** (a) Resistance (R_s) and recovery (R_c) of tree radial growth under mild,
 39 moderate, and severe wet years. (b) is the same as (a) but corresponds to drought
 40 events. R_s quantifies the growth deviation in the event year from the year prior to the
 41 wet/dry events, serving as an indicator of the event's immediate impact – values
 42 further from zero denote greater effects. Conversely, R_c measures the growth change
 43 from the event year to the year after wet/dry events, serving as an indicator of growth
 44 recovery – values further from zero denote more effective recovery. The cumulative
 45 effect of R_s and R_c ($R_s + R_c$), when closer to zero, suggests the minimal impact of the
 46 event. The wet/dry severities are calculated in the same way.

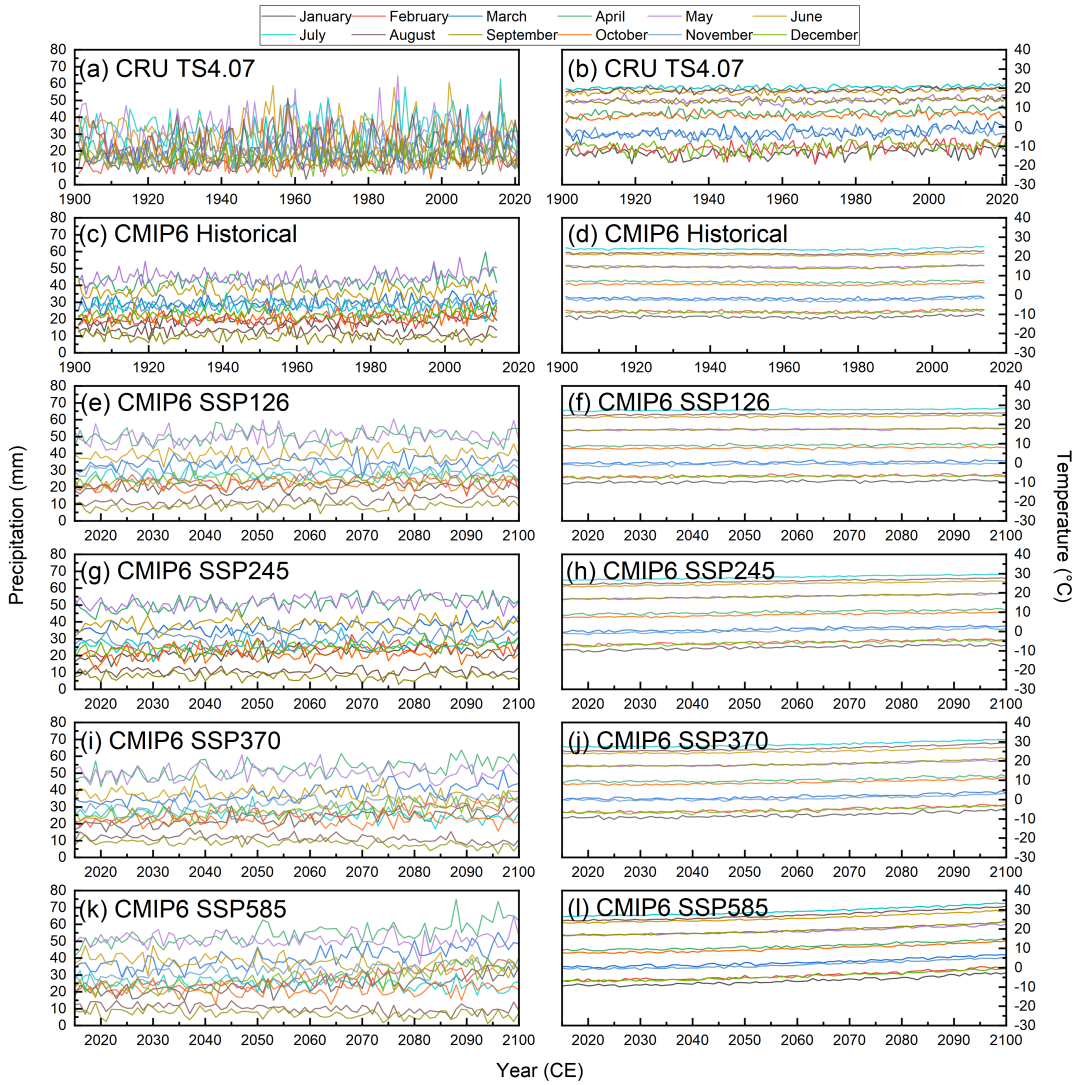
47



48

49 **Figure S4.** Comparisons of precipitation with the circum-low-latitude Indian Ocean,
 50 the circum-low-latitude central-east Pacific Ocean, the circum-low-latitude Atlantic
 51 Ocean, and the entire low-latitude regions, from the previous July to the current June
 52 for the original data **(a)** and first-order differences **(b)** of the observations. **(c-d)** are
 53 the same as (a-b) but are PC1.

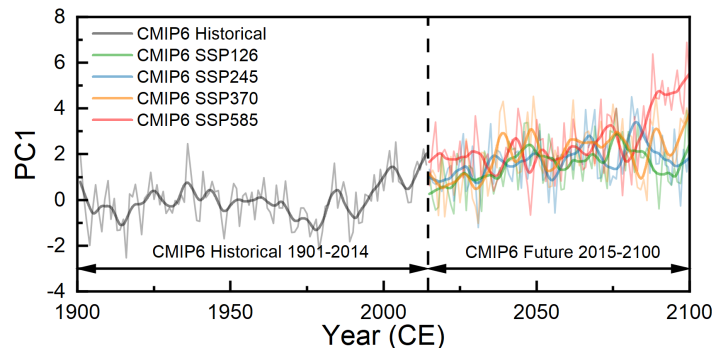
54



55

56 **Figure S5.** Monthly precipitation **(a)** and temperature **(b)** from 1901 to 2021 in CRU
 57 TS4.07 data (40°N – 50°N , 70°E – 90°E). **(c-d)**, **(e-f)**, **(g-h)**, **(i-m)**, and **(k-l)** are the
 58 same as **(a-b)**, but are historical simulations from 1901 to 2014, and future projections
 59 of SSP 1-2.6, SSP 2-4.5, SSP 3-7.0 & SSP 5-8.5 from 2015 to 2100, respectively, in
 60 downscaled and bias-corrected CMIP6 data.
 61

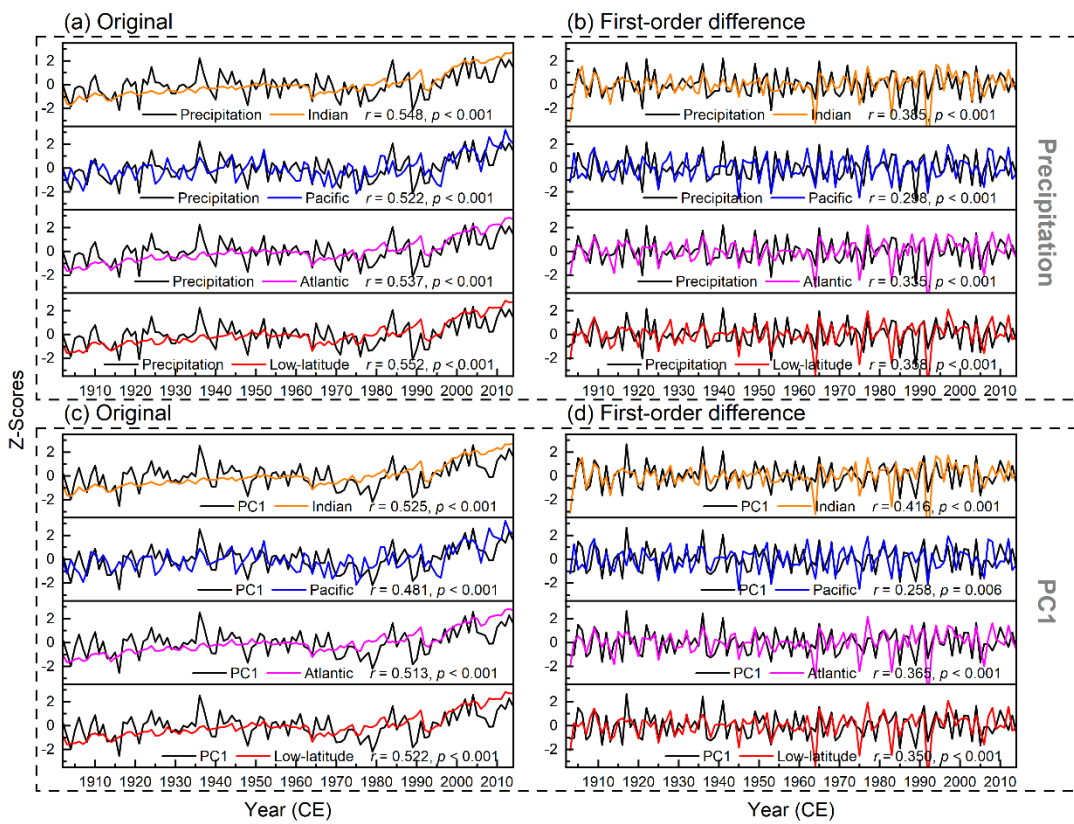
62



63

Figure S6. Simulated tree radial growth for historical and future scenarios (SSP 1-2.6, 64 SSP 2-4.5, SSP 3-7.0, and SSP 5-8.5) in CMIP6 based on VS-Lite. The simulated 65 values are scaled to the actual PC1, making the two directly comparable. The 9-year 66 low-pass filtered curves are shown in the plot.

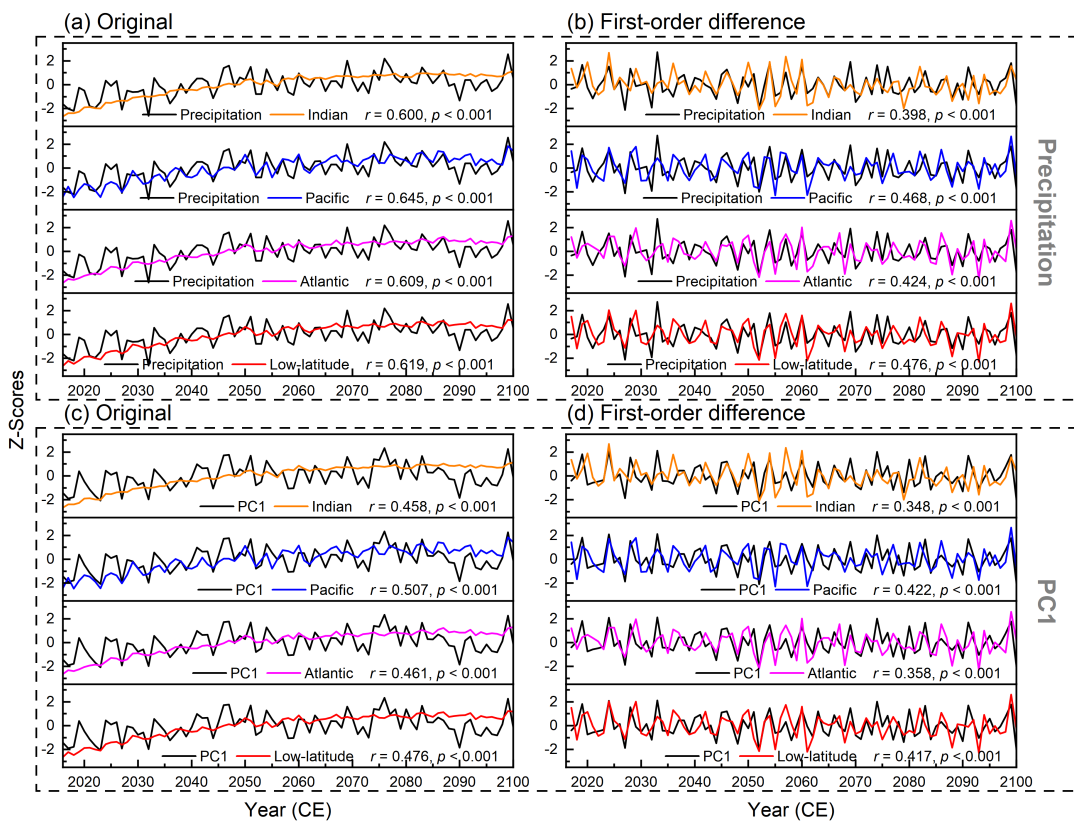
67



68

69 **Figure S7.** Same as Figure S3, but for the CMIP6 simulations for the historical
70 period.

71

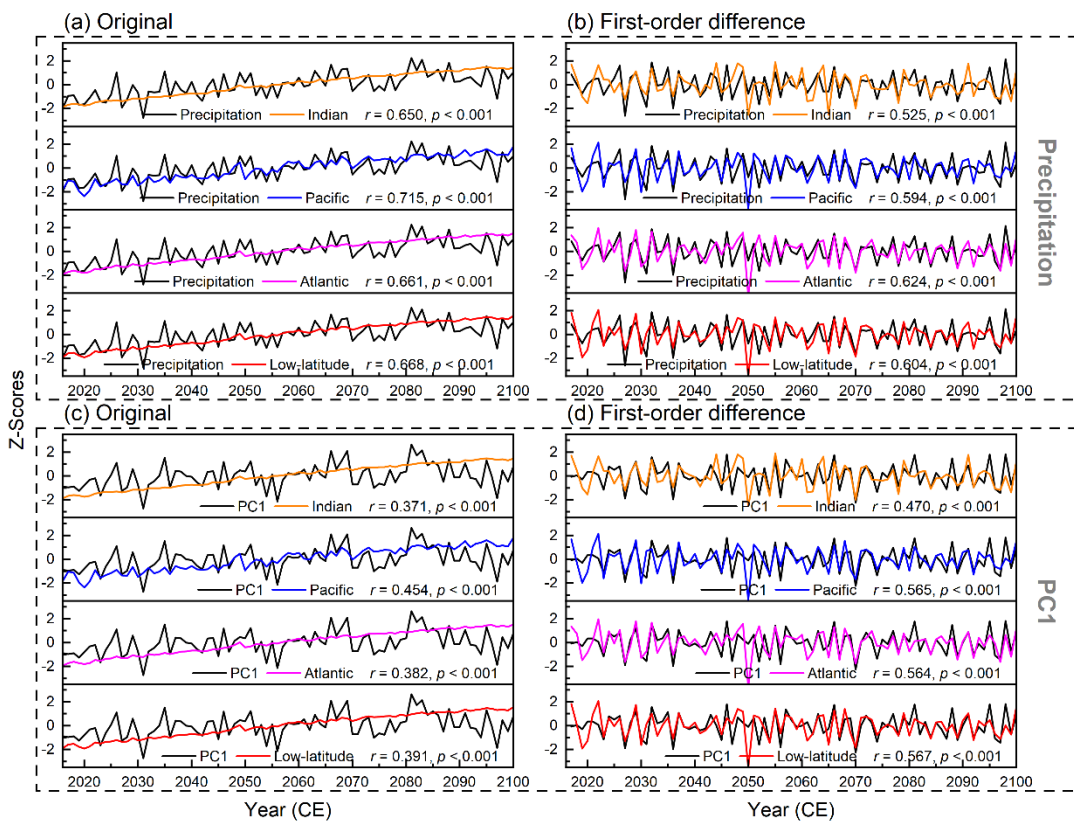


72

73 **Figure S8.** Same as Figure S3, but for the CMIP6 simulations for the future period

74 under the SSP 1-2.6 scenario.

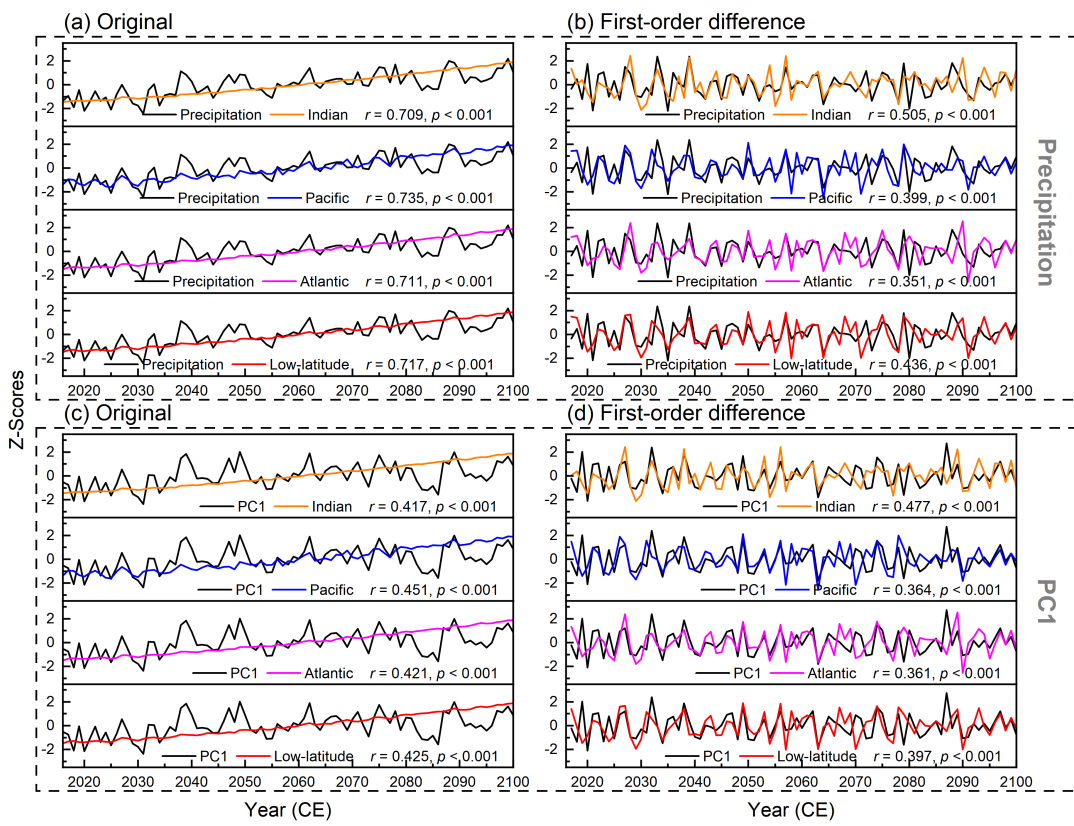
75



76

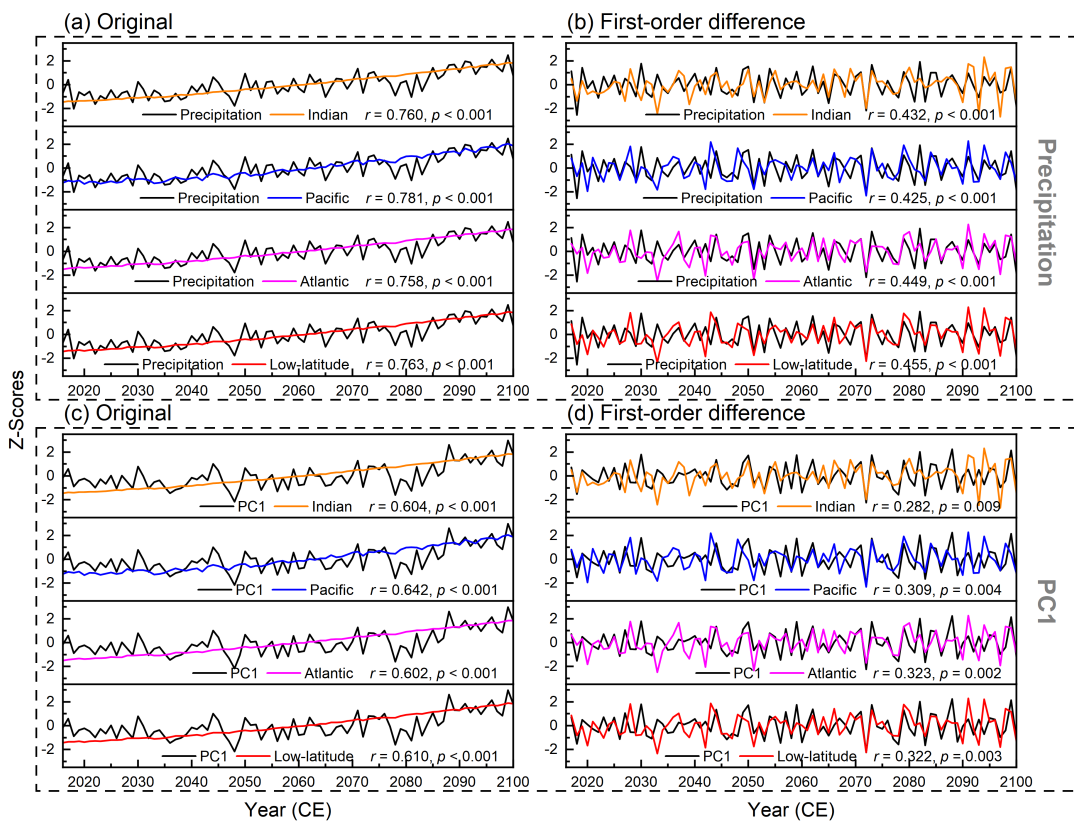
77 **Figure S9.** Same as Figure S3, but for the CMIP6 simulations for the future period
 78 under the SSP 2-4.5 scenario.

79



80

81 **Figure S10.** Same as Figure S3, but for the CMIP6 simulations for the future period
 82 under the SSP 3-7.0 scenario.
 83



84

85 **Figure S11.** Same as Figure S3, but for the CMIP6 simulations for the future period
 86 under the SSP 5-8.5 scenario.
 87

Table S1. Information about the sampling sites in the Central Asian alpine forests.

Source	Site code	Lon. (°E)	Lat. (°N)	Elevation (m)	Species	Latest year	Sources	Site code	Lon. (°E)	Lat. (°N)	Elevation (m)	Species	Latest year
1	chin007	88.15	43.93	1815	Spruce	2004	9	russ252	91.28	50.36	2170	Larch	2012
1	chin008	82.13	42.88	2763	Spruce	2004	9	russ254	89.59	50.24	2280	Larch	2012
1	chin009	82.15	43.07	2308	Spruce	2004	9	russ255	88.17	50.07	2100	Larch	2012
1	chin010	81.72	42.80	2593	Spruce	2004	9	russ257	88.14	49.39	2250	Larch	2011
1	chin011	82.87	43.15	1499	Spruce	2004	9	russ259	87.54	50.04	2250	Larch	2012
1	chin012	82.68	43.08	1710	Spruce	2004	10	AYS	86.38	43.57	2120-2250	Spruce	2003
1	chin013	86.72	43.72	1865	Spruce	2004	10	SRK	86.45	43.53	2450-2650	Spruce	2003
1	chin014	88.12	43.88	1913	Spruce	2004	10	KYS2	86.42	43.58	2065-2215	Spruce	2003
1	chin015	86.30	43.78	1878	Spruce	2004	10	WZG	86.65	43.72	2264-2350	Spruce	2009
1	chin033	87.92	43.77	1970	Spruce	2002	10	DOO	78.18	42.18	2800	Spruce	2013
1	chin034	88.02	43.80	2080	Spruce	2002	11	XBD	81.25	42.75	2600-2850	Spruce	2006
1	chin035	90.22	43.60	2250	Spruce	2002	11	KRK	81.83	42.88	2500-2645	Spruce	2006
1	chin036	90.10	43.60	2170	Spruce	2002	11	QLK	81.72	42.80	2500-2645	Spruce	2006
1	mong016	88.37	48.60	/	Larch	2004	12	BYX	90.45	43.60	2360	Spruce	2007
1	mong017	91.00	49.97	/	Larch	2005	13	JPK	82.90	44.10	2270-2492	Spruce	2009
1	mong018	90.98	49.48	/	Larch	2005	13	XHZ	83.25	44.37	2215-2390	Spruce	2009
1	mong019	90.97	47.10	/	Larch	2004	14	KYA	75.08	42.49	2600	Spruce	2015
1	mong020	88.87	48.27	/	Larch	2005	14	KYB	75.11	42.56	1990	Spruce	2015
1	mong024	88.50	48.50	/	Larch	2004	15	KA	75.35	42.52	1935	Spruce	2016
1	mong025	88.80	48.70	/	Larch	2004	15	TB	74.28	42.52	2020	Spruce	2015
1	mong029	91.43	49.87	/	Larch	1998	16	SJ	75.15	41.60	2800	Spruce	1995
2	kaz001	77.35	43.35	/	Spruce	2001	16	SK	76.43	41.67	2800	Spruce	1995
2	kyrg012	79.05	42.21	2827	Spruce	2005	16	KK	78.18	42.18	2850	Spruce	1995

2	kyrg013	79.46	42.15	2950	Spruce	2005	16	mong007	91.55	49.70	2000	Larch	1994
2	kyrg014	78.96	42.41	3010	Spruce	2005	16	mong009	91.57	49.92	2500	Larch	1998
2	kyrg015	79.45	42.15	3050	Spruce	2004	16	russ127	85.37	50.15	1750	Larch	1994
2	russ226	87.93	50.80	/	Larch	1998	16	russ129	85.63	51.00	1450	Larch	1994
2	russ227	88.10	49.62	/	Larch	2000	16	russ130	85.23	50.87	1450	Larch	1994
2	russ228	85.23	50.87	/	Larch	1995	16	russ133	87.68	50.50	1950	Larch	1994
2	russ229	87.83	50.30	/	Larch	2000	16	russ135	87.58	50.42	2000	Larch	1994
2	russ230	87.83	50.27	/	Larch	2000	16	russ136	85.23	50.87	1400	Larch	1994
2	russ231	87.28	49.17	/	Larch	2000	16	russ137	87.65	50.48	2150	Larch	1994
2	russ232	87.83	50.17	/	Larch	1999	16	russ139	85.37	50.15	1700	Spruce	1994
2	russ233	87.92	50.12	/	Larch	2000	16	russ140	84.98	50.65	1500	Larch	1994
2	russ234	87.48	50.48	/	Larch	1995	16	russ222	84.62	50.42	1898	Siberian Pine	2011
2	russ235	87.97	50.68	/	Larch	2000	17	BEL	82.96	45.78	2200-2252	Spruce	2008
3	TRK	86.70	48.45	1140-1160	Spruce	2013	17	TRX	82.53	45.74	1570-1735	Spruce	2008
4	XDY	88.87	43.80	2000	Spruce	2013	17	DLC	83.38	42.46	2750	Spruce	2014
4	WTG	89.17	43.67	2180	Spruce	2013	17	KCH	83.83	42.25	2620	Spruce	2014
4	KGY	89.62	43.53	2230	Spruce	2013	17	XLC	83.31	42.41	2228	Spruce	2014
4	DLY	90.23	43.60	2335	Spruce	2013	17	KTH	87.01	48.18	1168	Spruce	2019
4	LBY	92.35	43.48	2390	Spruce	2013	17	TLY	86.71	48.46	1050	Spruce	2019
4	LTY	92.88	43.53	2220	Spruce	2013	17	HDY	88.47	47.80	1610	Spruce	2019
4	SQG	93.40	43.47	2516	Spruce	2013	17	QBY1	87.61	48.16	/	Spruce	2019
5	TAS	93.83	43.25	2295-2363	Spruce	2009	17	QBY2	87.57	48.07	1315	Spruce	2019
6	DBX	87.28	43.45	2000-2160	Spruce	2008	17	QBY3	87.60	48.00	1157	Spruce	2019
6	YJD	87.08	43.13	2350-2550	Spruce	2008	17	TSMY	93.69	43.31	2686	Spruce	2019
6	MMK	86.93	43.43	2020-2134	Spruce	2008	17	BST	93.83	43.30	2291	Spruce	2019
6	STH	86.65	43.47	2030-2075	Spruce	2008	17	LWZ	89.78	43.56	2141	Spruce	2019

6	YJX	87.10	43.15	2370-2530	Spruce	2008	17	YJQ	87.08	43.13	2608	Spruce	2019
7	TLD	89.00	47.82	1260-1280	Spruce	2010	17	LLS	80.78	42.53	2439.25	Spruce	2006
7	XSK	88.98	47.70	1130-1280	Spruce	2010	17	AHY	81.06	42.71	2605.5	Spruce	2006
7	SEE	88.80	47.58	1155-1167	Spruce	2010	17	QEM	84.32	43.65	2348	Spruce	2021
7	XTK	89.10	47.68	1667-1700	Spruce	2010	17	ZKY	83.53	43.80	2159	Spruce	2021
7	KYS1	89.65	47.52	1590-1660	Spruce	2010	17	XTY	80.60	42.58	2726	Spruce	2020
7	DEN	89.63	47.42	1430-1460	Spruce	2010	17	AHY	81.38	42.57	2560	Spruce	2020
7	QBL	87.60	48.00	1204-1215	Spruce	2010	17	DKL	80.96	43.20	2355.37	Spruce	2021
8	TUY	77.00	43.05	2200	Spruce	2014	17	YGQ	82.22	42.91	2513.2	Spruce	2021
8	BAO	77.00	43.07	2125	Spruce	2014	17	KSR	81.72	42.80	2856	Spruce	2021
8	GOR	77.07	43.13	1868	Spruce	2014	17	XYN	83.21	43.26	2383	Spruce	2021
9	russ247	87.23	49.23	2200	Larch	2012	17	NZG	83.07	43.27	2118	Spruce	2021
9	russ248	87.02	49.20	2250	Larch	2010	17	QXY	82.68	43.05	1885	Spruce	2021
9	russ250	87.50	49.51	2250	Larch	2011	17	BTY	81.01	43.15	2163	Spruce	2021
9	russ251	86.57	49.36	2200	Larch	2011	17	BSF	81.04	43.42	2582	Spruce	2021

89 Note: Tree species are: Spruce – *Picea asperata* Mast.; Larch – *Larix gmelinii* (Rupr.) Kuzen.; Siberian Pine – *Pinus sibirica* Du Tour. Sample
 90 sources are specified as: 1-15 see corresponding references; 16 – Unknown specific references from the International Tree Ring Database
 91 (ITRDB); 17 – Tree-ring width chronologies published by our research group for the first time.

92

93 **Table S2.** Information about the 24 GCM models provided by CMIP6.

Model	Source	Accuracy (Lat×Lon)	Model	Source	Accuracy (Lat×Lon)
ACCESS-CM2	Australia	144×192	FGOALS-g3	China	80×180
ACCESS-ESM1-5	Australia	145×192	GFDL-ESM4	America	180×288
BCC-CSM2-MR	China	160×320	INM-CM4-8	Russia	120×180
CanESM5	Canada	64×128	INM-CM5-0	Russia	120×180
CAS-ESM2-0	China	128×256	IPSL-CM6A-LR	Europe	143×144
CESM2-WACCM	America	192×288	KACE-1-0-G	Korea	80×96
CMCC-CM2-SR5	Italy	192×288	MCM-UA-1-0	America	144×192
CMCC-ESM2	Italy	192×288	MIROC6	Japan	128×256
EC-Earth3	Europe	256×512	MPI-ESM1-2-HR	German	192×384
EC-Earth3-Veg	Europe	256×512	MPI-ESM1-2-LR	German	96×192
EC-Earth3-Veg-LR	Europe	160×320	MRI-ESM2-0	Japan	160×320
FGOALS-f3-L	China	192×288	NorESM2-LM	Norway	96×144

94

95

96 References

- 97 1 Cook, E.R., et al. Asian Monsoon Failure and Megadrought During the Last
98 Millennium. Science 328, 486-489 (2010).
99 <https://doi.org/10.1126/science.1185188>.

100 2 Ahmed, M., et al. Continental-scale temperature variability during the past two
101 millennia. Nat. Geosci. 6, 339-346 (2013). <https://doi.org/10.1038/NGEO1797>.

102 3 Chen, F., Yuan, Y. J., Zhang, T. W., Shang, H. M. Precipitation reconstruction for
103 the northwestern Chinese Altay since 1760 indicates the drought signals of the
104 northern part of inner Asia. Int. J. Biometeorol. 63, 455-463 (2016).
105 <https://doi.org/10.1007/s00484-015-1043-5>.

106 4 Chen, F., Shang, H. M., Yuan, Y. J. Dry/wet variations in the eastern Tien Shan
107 (China) since AD 1725 based on Schrenk spruce (*Picea schrenkiana* Fisch et
108 Mey) tree rings. Dendrochronologia 40, 110-116 (2016).
109 <https://doi.org/10.1016/j.dendro.2016.07.003>.

110 5 Chen, F. & Yuan, Y. J. Streamflow reconstruction for the Guxiang River, eastern
111 Tien Shan (China): linkages to the surrounding rivers of Central Asia. Environ.
112 Earth Sci. 75, 1049 (2016). <https://doi.org/10.1007/s12665-016-5849-1>.

113 6 Chen, F., Yuan, Y.J., Yu, S.L., Shang, H.M., Zhang, T.W. Tree-ring based
114 reconstruction of precipitation in the Urumqi region, China, since AD 1580
115 reveals changing drought signals. Clim. Res. 68, 49-58 (2016).
116 <https://doi.org/10.3354/cr01368>.

117 7 Chen, F., Yuan, Y.J., Davi, N., Zhang, T.W. Upper Irtysh River flow since AD
118 1500 as reconstructed by tree rings, reveals the hydroclimatic signal of inner
119 Asia. Clim. Change 139, 651-665 (2016).
120 <https://doi.org/10.1007/s10584-016-1814-y>.

121 8 Chen, F., Mambetov, B., Maisupova, B., Kelgenbayev, N. Drought variations in
122 Almaty (Kazakhstan) since AD 1785 based on spruce tree rings. Stoch. Environ.
123 Res. Risk Assess 31, 2097-2105 (2017).
124 <https://doi.org/10.1007/s00477-016-1290-y>.

- 125 9 Taynik, A.V. et al. Growth coherency and climate sensitivity of *Larix sibirica* at
126 the upper treeline in the Russian Altai-Sayan Mountains. *Dendrochronologia* 39,
127 10-16 (2016). <https://doi.org/10.1016/j.dendro.2015.12.003>.
- 128 10 Wang, H.Q., Chen, F., Ermenbaev, B., Satylkanov, R. Comparison of
129 drought-sensitive tree-ring records from the Tien Shan of Kyrgyzstan and
130 Xinjiang (China) during the last six centuries. *Adv. Clim. Chang. Res.* 8, 18-25
131 (2017). <https://doi.org/10.1016/j.accre.2017.03.004>.
- 132 11 Chen, F., Yuan, Y.J., Yu, S.L. Tree-ring indicators of rainfall and streamflow for
133 the Ili-Balkhash Basin, Central Asia since CE 1560. *Paleogeogr. Paleoceanogr. Paleoclimatol.*
134 *Paleoecol.* 482, 48-56 (2017). <https://doi.org/10.1016/j.palaeo.2017.05.029>.
- 135 12 Zhang, H.L. et al. A 422-Year Reconstruction of the Kaiken River Streamflow,
136 Xinjiang, Northwest China. *Atmosphere* 11, 1100 (2020).
137 <https://doi.org/10.3390/atmos11101100>.
- 138 13 Chen, F. et al. Ecological and societal effects of Central Asian streamflow
139 variation over the past eight centuries. *npj Clim. Atmos. Sci.* 5, 27 (2022).
140 <https://doi.org/10.1038/s41612-022-00239-5>.
- 141 14 Chen, Y.P. et al. Tree-ring perspective on past and future mass balance of the
142 glaciers in Tien Shan (Central Asia): An example from the accumulation area of
143 Tuyuksu Glacier, Kazakhstan. *Paleogeogr. Paleoceanogr. Paleoecol.* 625, 111696
144 (2023). <https://doi.org/10.1016/j.palaeo.2023.111696>.
- 145 15 Gao, Z.H. et al. Tree-ring based streamflow reconstruction of the Chu River in
146 Kyrgyzstan over the past 407 years. *Quat. Scineces* 42, 288-301 (2022).
147 <https://doi.org/10.11928/j.issn.1001-7410.2022.01.23>. (in Chinese)
- 148